

## Symbiosis, Morphology, and Phylogeny of Hoplonymphidae (Parabasalia) of the Wood-Feeding Roach *Cryptocercus punctulatus*

KEVIN J. CARPENTER,<sup>a</sup> ALES HORAK, LAWRENCE CHOW and PATRICK J. KEELING

Department of Botany, University of British Columbia, 3529-6270 University Boulevard, Vancouver, BC, Canada V6T 1Z4

**ABSTRACT.** Anaerobic cellulolytic flagellate protists of the hindguts of lower termites and the wood-feeding cockroach *Cryptocercus* are essential to their host's ability to digest lignocellulose. Many have bacteria associated with their surfaces and within cytoplasmic vesicles—likely important symbioses as suggested by molecular and other data. Some of the most striking examples of these symbioses are in the parabasalid family Hoplonymphidae, but little or no data exist on the structural aspects of their symbioses, their relationships with bacteria through different life-cycle stages, or their diversity and phylogenetic relationships in *Cryptocercus*. We investigated these areas in the hoplonymphid genera *Barbulanympha* and *Urinympa* from *Cryptocercus punctulatus* using light and electron microscopy, and analysis of small subunit rRNA. Microscopy reveals variation in density of bacterial surface symbionts related to life-cycle stage, a glycocalyx possibly important in bacterial adhesion and/or metabolite exchange, and putative viruses associated with bacterial surface symbionts. Patterning of surface bacteria suggests protists emerging from the resistant (dormant) stage are colonized by a small population of bacterial cells, which then divide to cover their surface. Additionally, cytoplasmic protrusions from the protist are covered by bacteria. Phylogenetic analysis rejects the monophyly of Hoplonymphidae, suggesting multiple origins or losses of these bacterial symbioses.

**Key Words.** Anaerobic protists, flagellates, Hoplonymphidae, morphology, Parabasalia, scanning electron microscopy, symbiosis, termites.

OF the many examples of microbial symbiosis, perhaps the most widely familiar and longest studied is that between lower termites (and the closely related wood-feeding cockroach *Cryptocercus*) and the anaerobic cellulolytic flagellate protists that inhabit their hindguts (Grassi 1917; Leidy 1877). A more recently studied, but arguably equally interesting and important symbiosis is found in the same environment that formed between many of these same protists and various bacteria, which are commonly found densely covering the cell surfaces and within cytoplasmic vesicles (Carpenter, Chow, and Keeling 2009; Cleveland and Grimstone 1964; Hongoh et al. 2008a; Noda et al. 2005; Radek, Hausmann, and Breunig 1992; Smith and Arnott 1974). Like the protists themselves, many of these bacterial symbionts are endemic to termite hindguts, and many occur only in association with a single protist host species within a single termite species (Ikeda-Ohtsubo et al. 2007; Noda et al. 2009). Some of these bacteria are hypothesized to represent novel phyla (Ohkuma and Kudo 1996; Stingl et al. 2005). The symbiotic nature and importance of these protist–bacterial associations is suggested by the production of special attachment structures by one or both of the partners (Bloodgood and Fitzharris 1976; Radek and Tischendorf 1999; Rother, Radek, and Hausmann 1999; Tamm 1980), the high degree of host–symbiont specificity (Ikeda-Ohtsubo et al. 2007; Noda et al. 2009), and the fact that in some termite species, over 70% of all bacterial cells in the hindgut occur in association with a protist (i.e. are not free-swimming; Noda et al. 2005). Hence, to a large extent, the termite's ability to survive on a diet of wood—which requires liberation of celluloses from lignin, enzymatic breakdown of the former, and also obtaining sufficient nitrogen (wood is very nitrogen poor)—is due not to a single symbiosis with an organism or taxonomic group of organisms, but rather due to many layers of symbioses, including protist–bacterial symbiotic consortia. Evidence indicates that, in general, these consortia function by the phagocytosis of ingested wood fragments, and enzymatic cellulose degradation by the protist (Cleveland et al. 1934; Nakashima, Watanabe, and Azuma 2002; Todaka et al. 2010; Yamin 1980). Byproducts of this include acetate and glucose, as well as waste

products, such as carbon dioxide and hydrogen gas (Ohkuma 2008). The acetate is the termite's sole carbon source, and glucose is transferred to bacterial symbionts (Hongoh et al. 2008a), which in turn are thought to provision the protist and the termite with amino acids and other essential nitrogenous nutrients (Hongoh et al. 2008a,b), in some cases using ammonia produced by nitrogen-fixing spirochetes in the gut. In addition to its unique and fascinating qualities from ecological and evolutionary perspectives, this complex and highly efficient system (Todaka et al. 2010) may be of practical interest for applications in producing biofuels (as well as hydrogen gas) from woody biomass.

The most dramatic examples of protist–bacterial symbioses in termite guts, and perhaps in any environment, are those involving members of Parabasalia, a monophyletic group of anaerobic flagellates with hydrogenosomes—H<sub>2</sub>-producing organelles derived from mitochondria that extract energy from conversion of pyruvate to acetate (Müller 1993). Parabasalia are characterized by numerous cytoskeletal synapomorphies, most notably the presence of parabasal bodies, which comprise unique proteinaceous parabasal fibers associated with Golgi bodies (Brugerolle and Lee 2000), from which the name of the group derives. Within Parabasalia, the hypermastigote cell form (which likely originated independently more than once—see Carpenter and Keeling 2007; Cepicka, Hampl, and Kulda 2010), occurs exclusively in termite/*Cryptocercus* hindguts, and many hypermastigotes have evolved large size and enormous structural complexity (Cleveland et al. 1934; Grassi 1917; Hollande and Carruette-Valentin 1971). Some species may have as many as 50,000 flagella forming stunning patterns through the repetition of various subsets of the basic cytoskeletal unit that defines the group (Cleveland et al. 1934). Although less well studied, hypermastigote parabasalids have also evolved a variety of equally dramatic associations with bacteria (Bloodgood and Fitzharris 1976; Carpenter et al. 2009; Radek et al. 1992). While some hypermastigote parabasalids have relatively few known bacterial symbionts (Carpenter, Horak, and Keeling 2010), others have extensive associations, containing up to 10<sup>5</sup> bacterial symbionts in the cytoplasm (Noda et al. 2005). Hypermastigotes of the family Hoplonymphidae accommodate extensive communities of bacterial symbionts, both on their surface and in cytoplasmic vesicles—in some cases having greatly modified their overall cellular morphology (e.g. by producing radiating vanes to which bacteria attach) to do so (Brugerolle and Bordereau 2004).

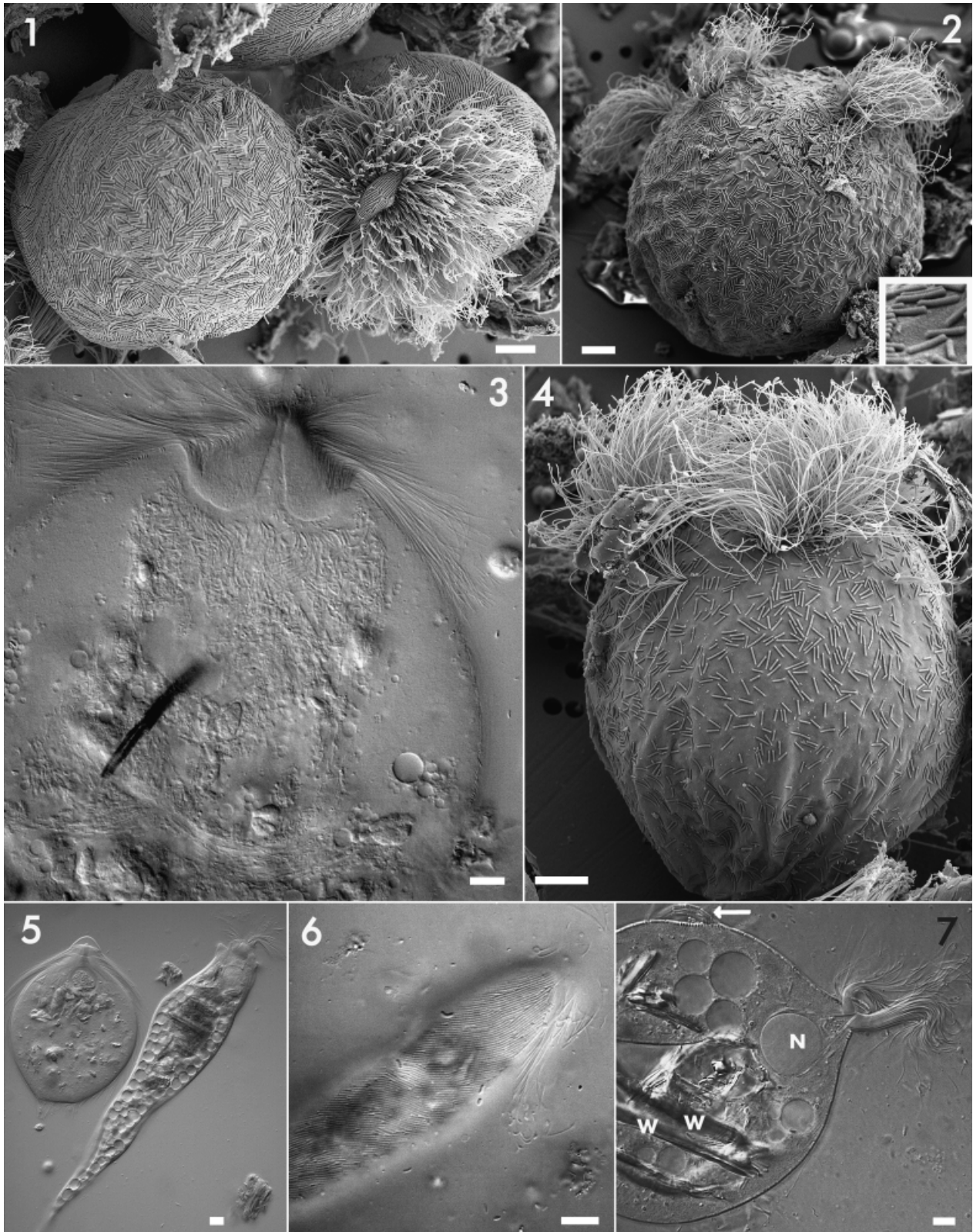
Hoplonymphidae are known from the hindguts of both lower termites and the wood-feeding cockroach *Cryptocercus*

<sup>a</sup>Present Address: Physical and Life Sciences Directorate, Lawrence Livermore National Laboratory, 7000 East Avenue, L-231, Livermore, California 94551, USA.

Corresponding Author: P.J. Keeling, Department of Botany, University of British Columbia, 3529-6270 University Boulevard, Vancouver, BC, Canada V6T 1Z4—Telephone number: +1 604 822 4906; FAX number: +1 604 822 6089; e-mail: pkeeling@mail.ubc.ca

*punctulatus* (Cleveland et al. 1934), suggesting the bacterial-protist associations are probably quite ancient, as are the microbial-insect associations (Carpenter et al. 2009; Ohkuma et al. 2009). Although the extensive nature of bacterial symbioses in

Hoplonymphidae has long been recognized (Bloodgood and Fitzharris 1976; Cleveland 1951; Noda et al. 2006), little or no data exist on the structural aspects of their symbioses (except for Bloodgood and Fitzharris 1976—discussed later), their



relationships with bacteria through different life-cycle stages, or their diversity and phylogenetic relationships in *Cryptocercus*. To explore these topics we have undertaken an extensive surface morphological and ultrastructural survey of the two genera of this family, *Barbulanympha* Cleveland and *Urinympha* Cleveland (Cleveland et al. 1934), which occur in the hindgut of Appalachian populations of the North American wood-feeding roach *C. punctulatus* using light (LM) and electron microscopy. In addition, we analyzed small subunit (SSU) rRNA from manually isolated cells as well as hindgut environmental samples to understand the diversity of this family and its phylogenetic relationships with other parabasalids, especially in light of morphological data from this and other studies on their bacterial symbiosis.

## MATERIALS AND METHODS

**Source of host organisms.** The wood-feeding cockroach *C. punctulatus* was sampled from several populations in the Appalachian Mountains of the eastern United States and generously provided by Christine Nalepa (North Carolina State University). Populations examined included: Bear Trap Gap, North Carolina; Log Hollow, North Carolina; Mount Collins, Tennessee; Mountain Lake, Virginia; South Mountains, North Carolina. GPS coordinates for these collection sites have been published (Eveaerts et al. 2008; Nalepa et al. 2002).

**Light and electron microscopy.** Live roaches were dissected and hindgut contents were suspended in Trager Medium U buffer (Trager 1934), examined by LM, and photographed with differential interference contrast illumination on a Zeiss (Oberkochen, Germany) Axioscope II light microscope. For scanning electron microscopy (SEM), hindgut material suspended in Trager Medium U buffer was fixed with OsO<sub>4</sub> vapor for 30 min followed by fixation in 1% (w/v) OsO<sub>4</sub> for 30 min. Fixed gut contents were pipetted onto a Millipore Isopore membrane filter (Billerica, MA) with 5- $\mu$ m pore size held in a Millipore Swinnex plastic cartridge affixed to a 10- $\mu$ l syringe. Material on the filters was rinsed in buffer and dehydrated in an ethanol series (50%, 70%, 90%, 2  $\times$  100%) for 10 min at each stage. Dehydrated material on filters was CO<sub>2</sub> critical point dried with a Balzers CPD 020 (Wetzlar, Germany) or Tousimis Autosamdri 815B Series A (Rockville, MD) critical point dryer. Dried filters were affixed to aluminum SEM stubs with double-stick carbon tape and coated with 5 nm of gold or gold-palladium using a Nanotech (Worcester, MA) SEM Prep2 or Cressington (Watford, UK) 208HR sputter coater. Material was examined and photographed in a Hitachi (Tokyo, Japan) S-4700 FESEM at 5 kV with working distance of 28 mm. Material for transmission electron microscopy (TEM) was prepared as described previously (Carpenter, Waller, and Keeling 2008). The two genera of Hoplonymphidae present—*Barbulanympha* and *Urinympha*—were distinguished using morphological characters from the original descriptions (Cleveland et al. 1934).

**Single cell isolation, and amplification and phylogenetic analysis of SSU rRNA.** Cells suspended in Trager Medium U were placed in a cavity slide and individual cells matching the description of either *Urinympha* or *Barbulanympha* were manually isolated using a micropipette. In the case of *Urinympha talea*, cells were observed to enlarge and become rounded after continued exposure to oxygen, and so only cells retaining their distinctive slender morphology and where the flagellar bundles beat in a strictly opposing fashion were isolated, so as to ensure no *Barbulanympha* was isolated with *Urinympha*. In the case of *Barbulanympha*, no attempt was made to isolate specific species in most isolations because, as Cleveland et al. (1934) observed, species distinctions are poorly defined and difficult to recognize even with fixed and stained specimens. The exception is *Barbulanympha ufalula*, which is considerably larger and more abundant than other species. In this case, single cells were identified and isolated. For both genera, single cells and pools of up to five cells were isolated, and DNA was purified using a single chloroform extraction followed by ethanol precipitation, as described (Keeling 2002). The SSU rRNA genes were amplified by rehydrating the DNA directly in a 10- $\mu$ l reaction volume using the primers 5'-GCGCTACCTGGTTGATCCTGCC-3' and 5'-TGATCCTTCTGCAGGTTACCTAC-3' and amplifying for 35 cycles with an annealing temperature of 45 °C and an extension time of 1.5 min. Products were separated by electrophoresis and cloned; multiple clones were sequenced on both strands. DNA was also purified from whole-gut contents and SSU rRNA genes amplified, cloned, and sequenced as described (Carpenter et al. 2009). New sequences were submitted to GenBank as accession numbers HQ636428–HQ626433.

**Phylogenetic analysis.** New sequences were added to an existing alignment (Carpenter and Keeling 2007; alignment available upon request), and phylogenetic relationships inferred using several methods. The maximum likelihood (ML) topology was inferred with RAxML 7.2.6 software (Stamatakis 2006) using GTR+GAMMA model of evolution. One hundred independent runs starting with randomized maximum parsimony trees were carried out and the topology with highest likelihood score chosen. The branching support was assessed using ML bootstrap analysis (RAxML, GTR+GAMMA, 1,000 replications) and Bayesian posterior probability. The latter was computed using MrBayes 3.1.2 (Ronquist and Huelsenbeck 2003) (GTR+GAMMA, 3,000,000 generations, priors set to default) and PhyloBayes 3.2 (Lartillot, Lepage, and Blanquart 2009) (CAT-GTR model, chain chains run until they converged). The monophyly of Hoplonymphidae was also tested with approximately unbiased (AU) and Shimodaira–Hasegawa (SH) tests. All sequences from the Hoplonymphidae were constrained to be monophyletic, and the tree then re-optimized using ML under the conditions described above, which resulted in the same topology as the ML tree, except with *Hoplonympha* at the base of the *Urinympha/Barbulanympha* clade. AU and

Fig. 1–7. Light and scanning electron micrographs of whole cells of *Barbulanympha* spp. and *Urinympha talea* from the wood-feeding cockroach *Cryptocercus punctulatus*. **1.** Scanning electron micrograph of *Barbulanympha* cells in two different orientations: anterior end facing upward, showing flagellated region (right cell); and posterior region facing upward, showing a dense covering of rod-shaped symbiotic surface bacteria (left cell). Because the anterior region is not visible, it is possible, but not likely (due to cell shape) that this cell is *U. talea*. **2.** Scanning electron micrograph of *Barbulanympha* cell in the process of division, showing two sets of flagellated regions, a sparse covering of symbiotic surface bacteria, and an apparent absence of glycocalyx. **Inset:** higher magnification view of the surface (an area of 5  $\mu$ m  $\times$  5  $\mu$ m). **3.** Light micrograph of a *Barbulanympha* cell showing bilaterally symmetric semiconical, anterior flagellated region. **4.** Scanning electron micrograph of a side view of *Barbulanympha* showing anterior flagellated region at top, and posterior region with rod-shaped symbiotic surface bacteria. **5.** Light micrograph of *U. talea* (cell on right [cell on left is *Trichonympha* sp.]) showing elongate form and numerous large cytoplasmic vacuoles. **6.** Light micrograph of *U. talea* showing elongate form and a dense covering of rod-shaped symbiotic surface bacteria. **7.** Light micrograph of *U. talea* showing two narrow, distinct anterior flagellated regions (at right), a large nucleus (N), ingested wood fragments (W), a cytoplasmic protrusion covered by bacteria (arrow), and numerous large cytoplasmic vacuoles. Scale bars = 10  $\mu$ m.

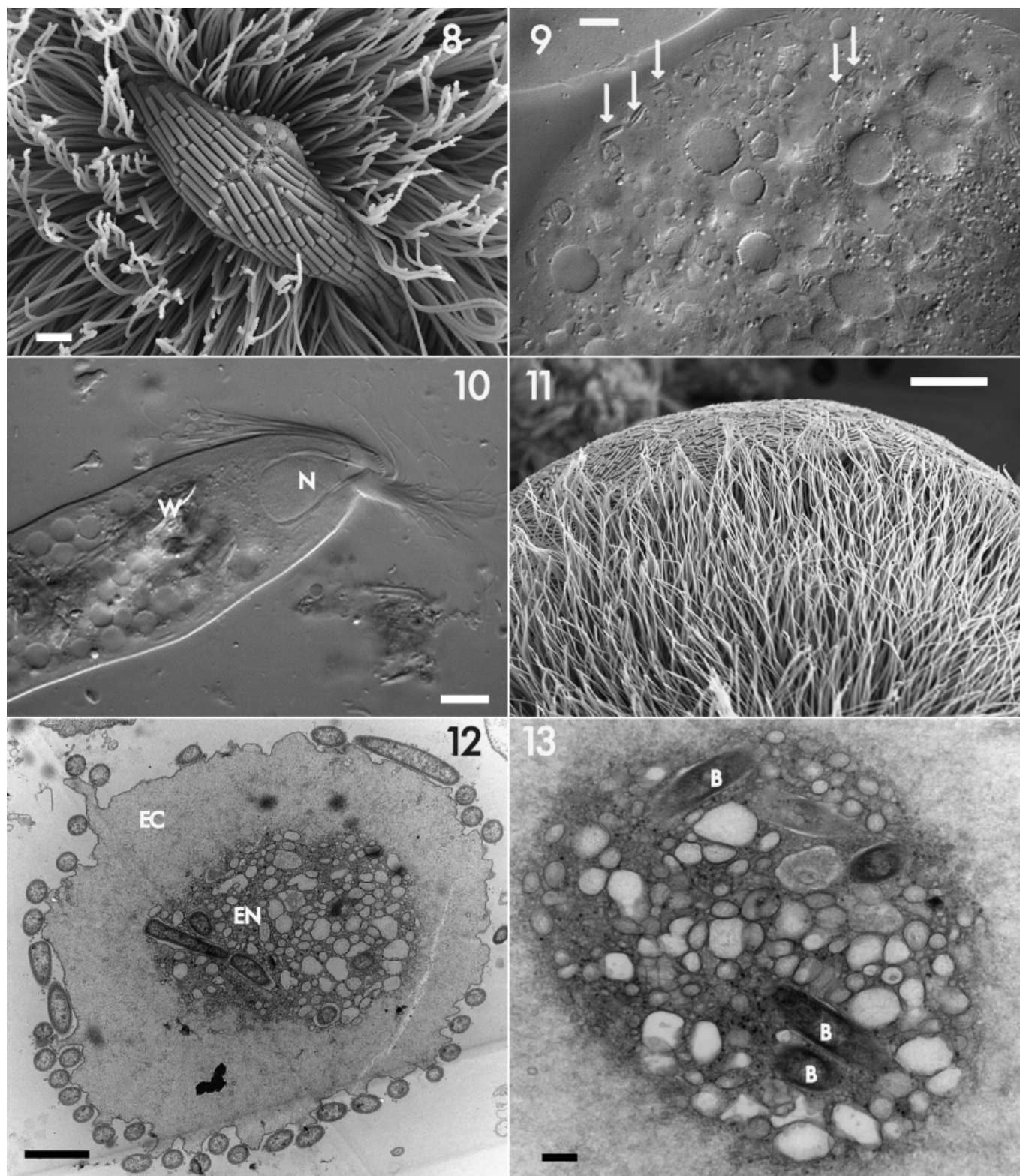
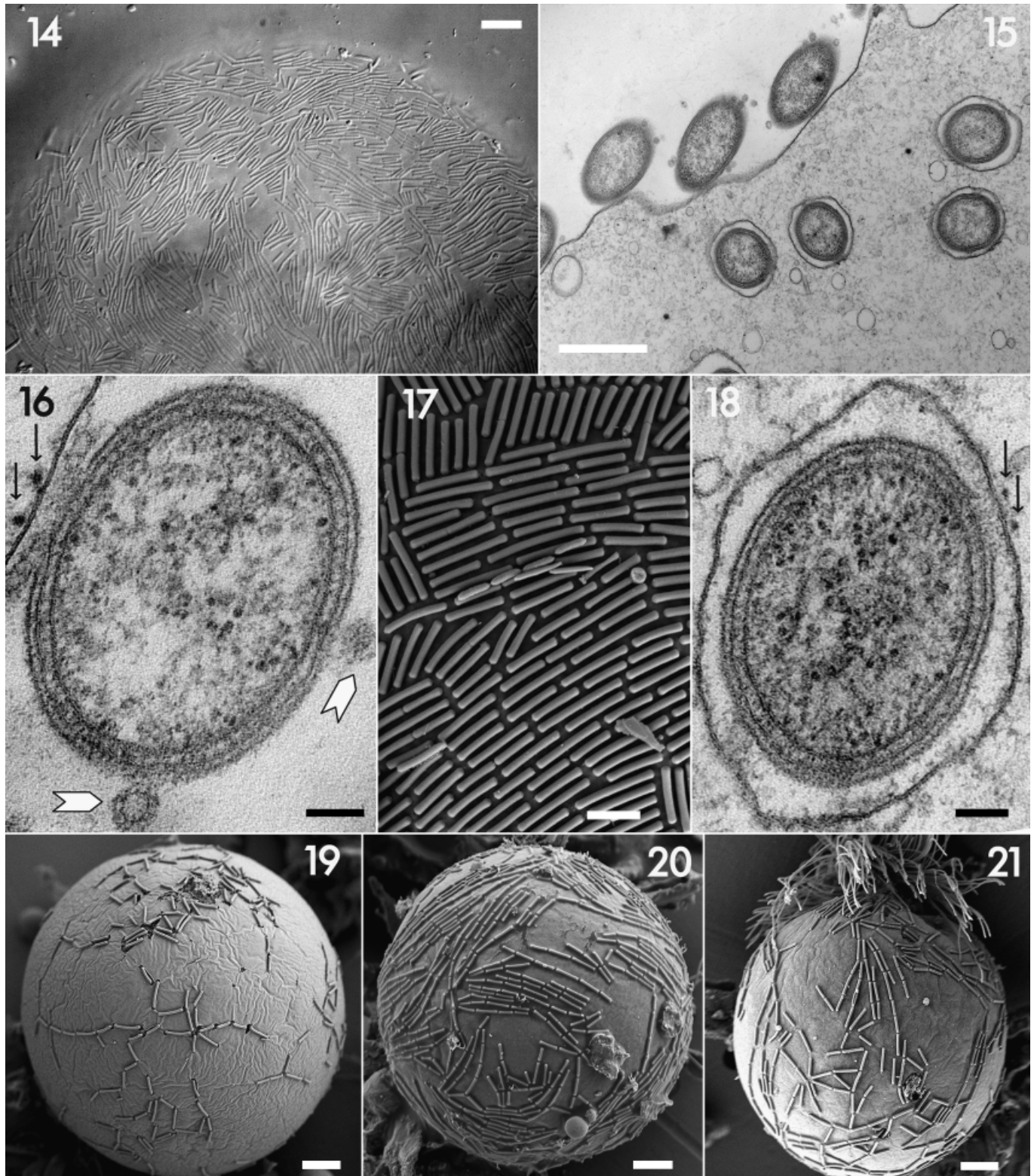


Fig. 8–13. Light and scanning and transmission electron micrographs of *Barbulanympha* spp. and *Urinympha talea* from the wood-feeding cockroach *Cryptocercus punctulatus*. **8.** Scanning electron micrograph of the anterior end of *Barbulanympha* sp. showing the operculum covered with rod-shaped symbiotic surface bacteria surrounded by flagella. **9.** Light micrograph of the posterior end of *Barbulanympha* sp. showing rod-shaped bacteria (arrows). **10.** Light micrograph of the anterior end of *U. talea* showing two distinct flagellar regions, nucleus (N), wood fragments (W), and numerous large cytoplasmic vacuoles. **11.** Scanning electron micrograph of a portion of the anterior pole of a *Barbulanympha* sp. cell showing detail of flagella and symbiotic surface bacteria. **12.** Transmission electron micrograph of a cross-section of a *Barbulanympha* or *Urinympha* cell (likely the latter due to the relatively small diameter) showing rod-shaped symbiotic surface bacteria, similar bacteria within cytoplasmic vesicles, and the clear zonation of the cell into interior endoplasm (EN), which houses all organelles, and the outer ectoplasm (EC). **13.** Transmission electron micrograph showing detail of the endoplasm with symbiotic bacteria in vesicles (B), and ectoplasm of a *Barbulanympha* or *Urinympha* cell. Scale bars: Fig. 8, 12 = 2  $\mu$ m; 9, 10, 11 = 10  $\mu$ m; 13 = 500 nm.

SH tests were carried out on the original tree and this alternative using CONSEL (Shimodaira 2002; Shimodaira and Hasegawa 2001). Both sets of tests rejected the monophyletic Hoplonyphidae.

## RESULTS

**Overall cell morphology and distribution.** Members of both genera are large (Fig. 1–7), ranging from 62 to 159  $\mu\text{m}$  long by



69–142  $\mu\text{m}$  wide for *Barbulanympha* (Fig. 1–4) and from 117 to 315  $\mu\text{m}$  long by 23–142  $\mu\text{m}$  wide for *Urinympa* (Fig. 5–7). *Barbulanympha* is typically spheroidal (Fig. 1–7), while *Urinympa* in fresh preparations assumes an elongate form (Fig. 5, 6, 10), but can also appear spheroidal in less optimum conditions (Fig. 7). The cytoplasm of *Urinympa* is also distinctive because of the presence of numerous large vacuoles (Fig. 5, 7), which are present, but neither as common nor as pronounced in *Barbulanympha* (Fig. 3, 9). The anterior end of the cell in both genera is bilaterally symmetric, comprising two identical flagellated zones, each bearing hundreds or thousands of flagella (Fig. 1–3, 5, 7). These zones in *Barbulanympha* are very broad and, although semiconoidal in shape (Fig. 3), give the appearance of a continuous ring of flagella (Fig. 1, 8), while those in *Urinympa* form two smaller, more widely separated areas with fewer flagella overall (Fig. 5, 7, 10). As observed in live cells with LM, flagella in these two genera are distinct behaviorally as well: flagella in *Barbulanympha* appear to move more or less independently, giving the overall impression of swaying, while flagella from each of the two zones in *Urinympa* tend to move in unison and beat in opposition to each another, giving the impression of two super flagella, each composed of hundreds of individual flagella (e.g. Fig. 7, 10).

Other features of finer scale morphology are shown in Fig. 8–13. These include the operculum, the anterior most cap-like structure situated between the two flagellated zones (Fig. 8, 10), and the distinct division of cytoplasm into inner endoplasm (containing all organelles) and outer ectoplasm, as seen in transverse section in TEM (Fig. 12, 13). A large nucleus contained in a membranous nuclear sleeve is present in the anterior portion of these cells (Fig. 7, 10).

*Barbulanympha* was present and generally abundant in all *Cryptocercus* individuals of all populations sampled, as observed by LM and SEM. In contrast, *Urinympa* was observed less commonly and, although present in all populations, did not appear to be present in LM observations of all individuals—a finding consistent with the original description of the genera (Cleveland et al. 1934). Although they are easily distinguishable in LM, the characteristics that specify *Urinympa* (e.g. flagellar beat patterns, the shape of anterior flagellated regions, the presence and nature of large cytoplasmic vacuoles, and the three dimensional shape of the cell) are not readily observable with TEM or SEM. In addition, because *Urinympa* only appeared in certain individuals, it was absent in at least some of the material prepared for SEM and TEM. Accordingly, although many cells we observed in SEM or TEM preparations could be confidently attributed to *Barbulanympha*, no cells unequivocally conformed to the description of *Urinympa*. The flagellated regions were usually not observed in SEM preparations, as these cells have a tendency to orient downward, thus obscuring the anterior cell pole (e.g. left cell, Fig. 1). Likewise, we did not observe any TEM sections of cells with large vacuoles that could not potentially be those of *Barbulanympha*.

Hence, some cells in SEM and TEM can be attributed to *Barbulanympha*, but others cannot unequivocally be assigned to either genus. It is possible that some such cells may in fact represent *Urinympa*, although the fact that *Urinympa* is considerably less common than *Barbulanympha* (confirmed with LM), suggests that most of these cells are *Barbulanympha*.

**Symbioses with bacteria.** Nearly all *Barbulanympha* and *Urinympa* trophozoites (i.e. the active, feeding stage) were observed to be covered with a dense monolayer of rod-shaped bacteria that range from  $\sim 1$  to 3  $\mu\text{m}$  in length and appear in TEM to have Gram-negative-type cell walls (Fig. 1, 2, 4, 6, 8, 11, 12, 14, 17, 22). In LM they appear as dense striations on surfaces (Fig. 6, 14) or as a surface monolayer in section (Fig. 7). Molecular data from a previous study place these bacteria in the order Bacteroidales (Noda et al. 2006). These bacterial cells are often associated with two 20-nm-diam. dots just under the plasma membrane of the host cell (arrows, Fig. 16; Fig. 23); these have been identified as specialized rod-like attachment structures (seen in cross section here) produced by the protist (Bloodgood and Fitzharris 1976). In most cells, bacteria are present on the entire cell surface including the operculum (Fig. 8), and are absent only from the flagellar emergence points. Morphologically identical bacterial cells are also present within vesicles scattered throughout the cytoplasm (Fig. 12, 13, 15, 18) that are associated with identical attachment structures (arrows, Fig. 18). These bacteria, which, like the surface bacteria, are clearly visible in LM (e.g. Fig. 9), are thought to be derived from surface bacteria by phagocytosis (Bloodgood and Fitzharris 1976), but we saw no evidence of their being degraded.

Numerous circular structures approximately  $\sim 90$  nm in diam.—possibly viruses—were observed with TEM attached to, or near, many surface bacteria (Fig. 15, 16 [arrowheads], 23). We did not observe these putative viruses to be associated with bacteria within protist cytoplasmic vesicles.

Our SEM data suggest that density of surface bacteria varies with protist life-cycle stage—with a loss of many (but not all) surface bacteria occurring in protist host cells undergoing division (Fig. 2), and in the formation of resistant cells that form in response to insect molting (Fig. 19–21).

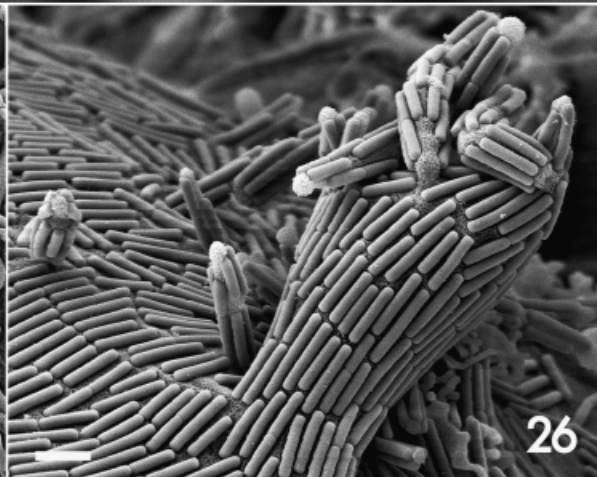
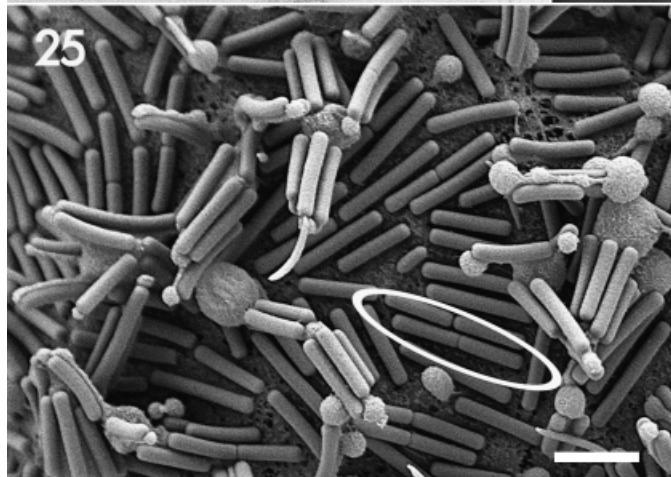
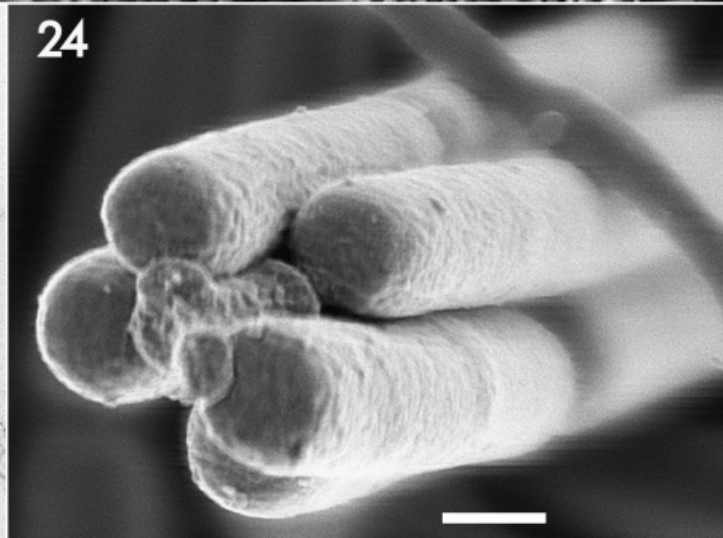
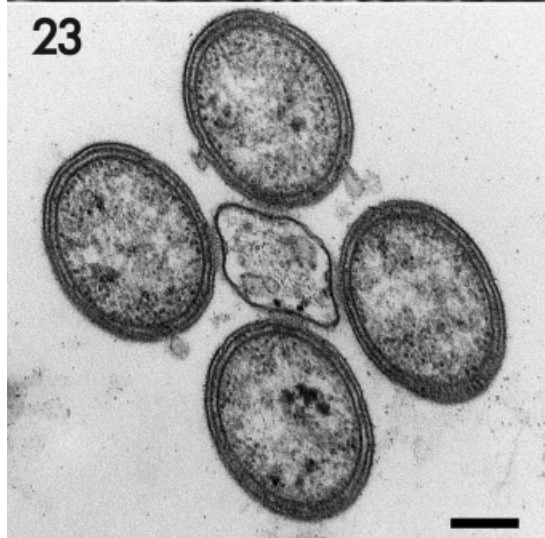
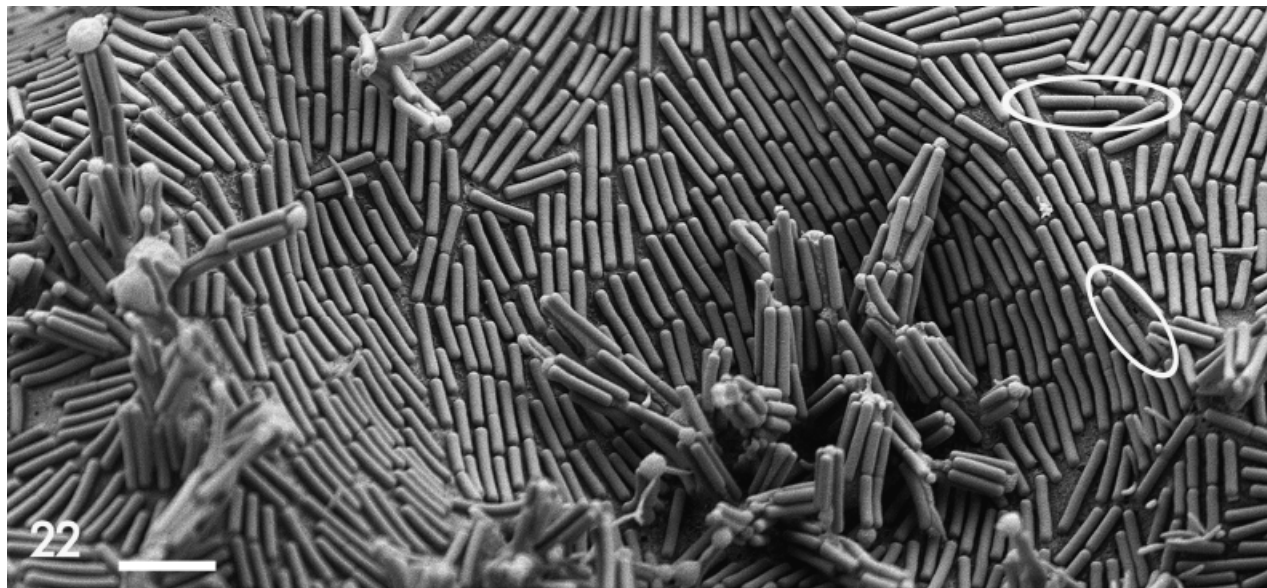
Another feature revealed by SEM is the presence of a spongy glycocalyx on the *Barbulanympha* cell surface (Fig. 8, 22, 25, 26). Examination with TEM shows this as well, and in addition suggests a thickening of the glycocalyx between the protist plasma membrane and the outer membrane of the bacterial surface symbiont (Fig. 15, 16, 23). This can also be seen in bacterial cells held within cytoplasmic vesicles (Fig. 18). However, here it is not as prominent, and may be in the process of being degraded.

It is also possible that the glycocalyx functions in binding bacterial cells to the protist cell surface, perhaps working in conjunction with the specialized attachment structures produced by the protist. In resistant cells (Fig. 19–21) and dividing cells (Fig. 2 and inset)—both of which exhibit sparse coverings of surface

Fig. 14–21. Light and scanning and transmission electron micrographs of bacterial surface symbionts and endosymbionts of *Barbulanympha* spp. and *Urinympa talea* from the wood-feeding cockroach *Cryptocercus punctulatus*. 14. Light micrograph of a *Barbulanympha* cell covered with bacteria, most of which appear more haphazardly distributed. 15. Transmission electron micrograph of a *Barbulanympha* or *Urinympa* cell showing symbiotic surface bacteria, as well as morphologically identical bacteria within cytoplasmic vesicles. 16. Transmission electron micrograph of a symbiotic surface bacterium of a *Barbulanympha* or *Urinympa* cell showing Gram-negative cell wall, associated viruses (arrowheads), a thickened glycocalyx between the bacterium and the host protist, and two specialized attachment structures produced by the protist (arrows). 17. Scanning electron micrograph of symbiotic surface bacteria of a *Barbulanympha* or *Urinympa* cell showing linear arrangement of cells, indicative of bacterial cell division. 18. Transmission electron micrograph of a bacterial endosymbiont held in a vesicle of a *Barbulanympha* or *Urinympa* cell. Note the attachment structures, which are morphologically identical to the ones associated with surface bacteria. 19, 20. Scanning electron micrographs of resistant forms of *Barbulanympha* and/or *Urinympa* cells. Note the spherical form, reduced size (compared with trophozoites), and linear arrangement of symbiotic surface bacteria. 21. Scanning electron micrograph of a resistant form of *Barbulanympha* or *Urinympa* emerging from the resistant stage to form a trophozoite. Note the linear arrangement of symbiotic surface bacteria and the new flagella being formed (at top). Scale bars: Fig. 14 = 10  $\mu\text{m}$ ; 15 = 1  $\mu\text{m}$ ; 16, 18 = 100 nm; 17 = 2  $\mu\text{m}$ ; 19–21 = 5  $\mu\text{m}$ .

bacteria—the cell surface appears smooth, possibly indicating a reduction or loss of glycocalyx. Cleveland et al. (1934) also noted changes in the cell surface, which they termed the “cuticle,” occurring in the formation of resistant cells; these changes presu-

ably allow the cell to survive in the aerobic environment outside the insect (i.e. before they are transferred to newly hatched nymphs). Hence, in addition to the density of surface bacteria, the glycocalyx also varies with life-cycle stage, altogether



suggesting that there is a functional relationship between its presence and density of surface bacteria. This is also supported by the fact that the one trophozoite cell we noted to have sparse covering of surface bacteria also had a smooth surface (Fig. 4). It is possible that this cell may be preparing to divide or form a resistant cell.

Both SEM and LM reveal variable patterns of bacterial cell arrangement on the protist cell surfaces, ranging from somewhat random (Fig. 1 [left cell], 14), to the more common highly ordered configurations comprising (in part) numerous rows of cells arranged end to end (Fig. 8, 17, 19–21, 22, 26). The linear patterns follow the bacterial plane of division (i.e. perpendicular to their long axis), and are seen on both trophozoites as well as resistant cells, although the clearest examples were observed on the latter (Fig. 19–21).

Perhaps the most dramatic manifestation of the division of the bacterial symbionts is the appearance in many cells of cytoplasmic protrusions of extruded protist cytoplasm covered with surface bacteria (Fig. 22–26). These structures can be seen in both *Barbulanympha* and *Urinympha* in LM (e.g. arrow Fig. 7), however, they are more easily interpreted in SEM (Fig. 22, 24, 25, 26) and TEM (Fig. 23).

The cytoplasmic protrusions range up to 10  $\mu\text{m}$  long and may bear from several to as few as two bacterial cells around the circumference (Fig. 22–26). These cytoplasmic protrusions are also visible in TEM, which shows attachment structures (identical to those described previously) under the protist plasma membrane adjacent to attached bacteria (Fig. 23). Interestingly, a single tower is evident in one previously published TEM micrograph (Bloodgood and Fitzharris 1976: figure 5B), although the authors did not comment on it. On one cell, the protrusions were present at the end of a larger club-like structure (Fig. 26), thus representing two levels of branching.

**Diversity and relationship of *Barbulanympha* and *Urinympha* according to SSU rRNA phylogeny.** Cleveland et al. (1934) were uncertain of the number of species of *Barbulanympha* or what the affinities of *Barbulanympha* and *Urinympha* might be, but suggested there were four species of *Barbulanympha*, and that *Urinympha* was its sister genus. He also suggested both were related to another species with a dense coating of surface symbionts, *Hoplonympha*, which together with *Rhynchonympha* from Pacific coast populations of *C. punctulatus* comprise the Hoplonymphidae (Cleveland et al. 1934). We examined the number of species of *Barbulanympha* by isolating several single cells and small groups of *Barbulanympha* cells, as well as several independent isolations of *U. talea*, both of which were also isolated by an independent study during the course of this work (Ohkuma et al. 2009). For *Barbulanympha*, five distinct sequence types were recovered (Fig. 27), one of which was not described by Ohkuma et al. (2009). A single sequence type was consistently recovered from *U. talea*, suggesting the identification of a single species was correct. *Urinympha* was found to be the sister group to *Barbulanympha*, though the monophyly of *Barbulanympha* to the exclusion of *Urinympha* was only weakly supported (Fig. 27).

Phylogenetic analysis does not support the monophyly of Hoplonymphidae; rather, *Hoplonympha* is weakly supported as the sister to a clade comprising two major branches: a clade of *Barbulanympha* and *Urinympha*, and a clade comprising the spirotrichosome *Leptospironympha* and the eucomonymphids *Eucomonympha*, *Pseudotriconympha*, and *Teranympha* (Fig. 27). The monophyly of *Hoplonympha* with *Barbulanympha* and *Urinympha* was rejected by AU and SH tests at the 1% confidence level. In some previous analyses the Hoplonymphidae were found to be monophyletic (e.g. Ohkuma et al. 2009), but this was before the characterization of the SSU rRNA from *Leptospironympha* (Carpenter et al. 2010), which likely accounts for this discrepancy.

## DISCUSSION

**Putative viruses.** Given the high degree of endemism in termite/*Cryptocercus* guts, with many protist species found only in one species of termite (Noda et al. 2007; Yamin 1979), and many bacteria found in symbiotic association with only one species of protist (Ikeda-Ohtsubo et al. 2007; Noda et al. 2009; Ohkuma 2008), it may be that these viruses represent novel types endemic to these systems as well.

**Symbioses with bacteria.** In forming a resistant stage, the trophozoite discards all flagella, reduces extranuclear organelles, becomes reduced in size, assumes a spherical shape, and undergoes changes in the cell surface (Cleveland et al. 1934).

The fact that at least some bacteria remain attached to resistant forms and dividing cells suggests that the specialized attachment structures formed by the protist are strong, and that at least some are able to withstand the changes in cellular shape, size, and surfaces that occur during these processes. The strength of such specialized attachment structures has been noted in *Barbulanympha* (Bloodgood and Fitzharris 1976), as well as in other parabasalid termite gut symbionts (Radek and Tischendorf 1999) in experiments that attempted to disrupt the connection using a variety of chemical and physical treatments. Moreover, it is thought that the rod-shaped surface symbionts are highly specific to their protist host species, and are not found free-swimming in the gut (Ikeda-Ohtsubo et al. 2007; Noda et al. 2009; Ohkuma 2008). These observations raise interesting questions about how the surface is colonized and perhaps periodically cleared of symbionts. One intriguing possibility is that at certain times in the life cycle of *Barbulanympha* the surface is cleared but bacteria are retained in vesicles, and that recolonization of the surface originates from these intracellular relicts.

That similar glycocalyx thickenings are seen in other parabasalid, as well as oxymonad termite gut symbionts bearing surface symbiotic bacteria (Brugerolle and Bordereau 2004; Radek and Tischendorf 1999) suggests a role for this structure in attachment or perhaps mediating exchange of metabolites between the symbiotic partners. Indeed, unless it is possible for metabolite exchange to occur via the special attachment structures produced by the protist, the glycocalyx appears to be the only route through

Fig. 22–26. Scanning and transmission electron micrographs of cytoplasmic protrusions comprising extruded protist cytoplasm and symbiotic surface bacteria of *Barbulanympha* and/or *Urinympha* cells from the wood-feeding cockroach *Cryptocercus punctulatus*. 22. Scanning electron micrograph of the surface of a *Barbulanympha* or *Urinympha* cell showing numerous protrusions. Note the linear arrangement of many bacterial cells and the evidence of recent bacterial cell division in the form cells with incompletely formed cross-walls (i.e. shallow transverse furrows encircled by ellipses). 23. Transmission electron micrograph of a cross section of a cytoplasmic protrusion showing protist cytoplasm and plasma membrane with thickened glycocalyx at bacterial attachment sites, surrounded by four bacterial surface symbionts showing Gram-negative walls and associated viruses. Note the two specialized attachment structures (as in Fig. 16, 18) in the protist cytoplasm adjacent to the bottom bacterial cell. 24. Scanning electron micrograph of the distal end of a protrusion showing protist cytoplasm/plasma membrane surrounded by four bacterial cells. 25. Detail of a *Barbulanympha* or *Urinympha* cell surface showing protrusions of various shapes, most of which have caps of glycocalyx, or glycocalyx-covered material. Note also the cells undergoing division (ellipse). 26. Detail of a *Barbulanympha* cell surface showing a club-like extension branching into smaller cytoplasmic protrusions. Scale bars: Fig. 22 = 3  $\mu\text{m}$ ; 23 = 100 nm; 24 = 300 nm; 25, 26 = 2  $\mu\text{m}$ .

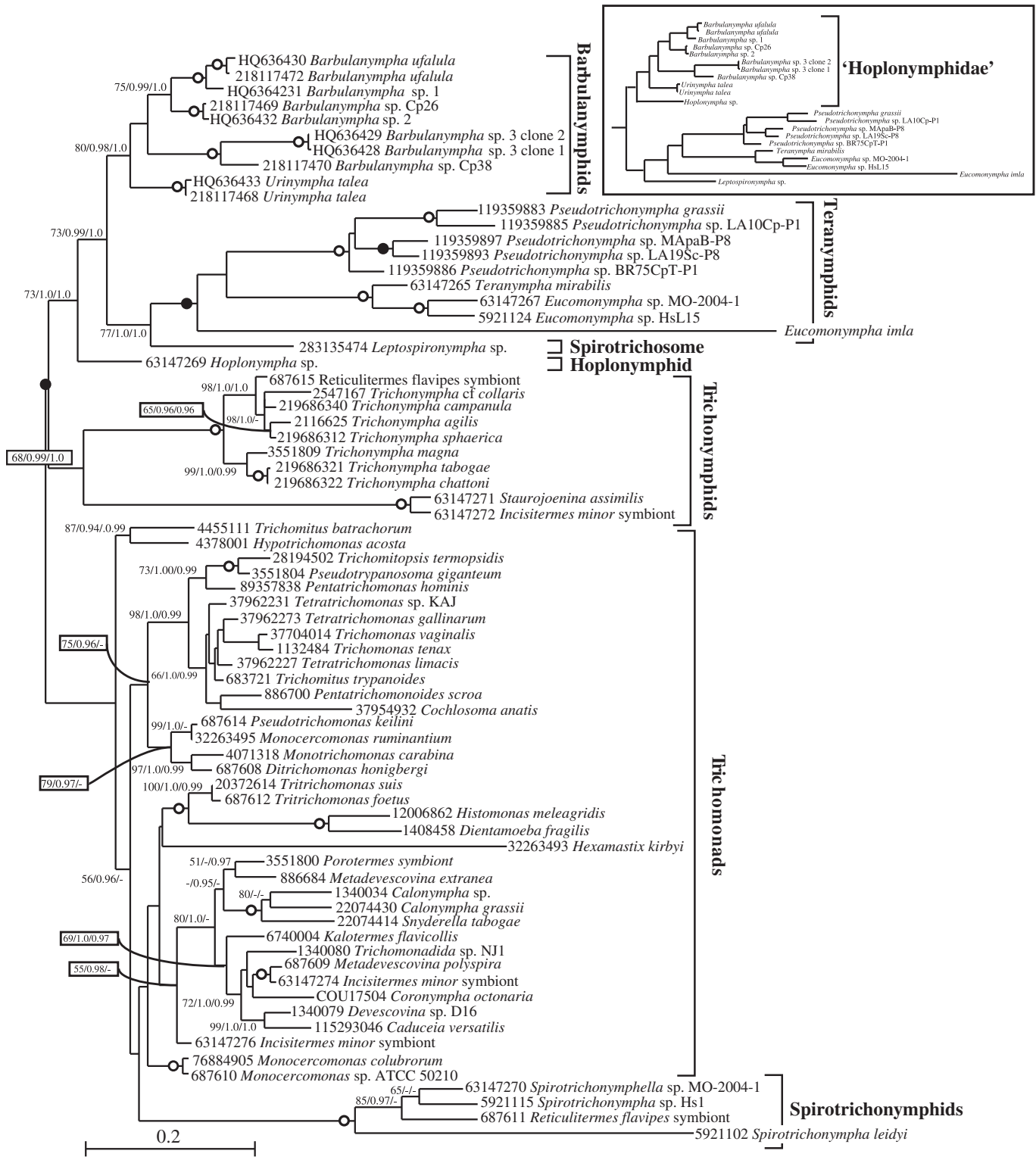


Fig. 27. Maximum likelihood (ML) phylogeny of parabasalid small subunit (SSU) rRNA sequences. Taxon names include GenBank ID followed by scientific name, with higher level groups indicated by brackets and names to the right. Numbers at nodes correspond to support values from (left to right) ML, MrBayes, and PhyloBayes (see “Materials and Methods” for details). Open circles denote absolute support (i.e. 100/1/1), full circles show strong support (>90, >0.95, >0.95). The hypothesized Hoplonymphidae are not monophyletic because barbulanymphids and hoplonymphids do not branch together in any of our analyses. The monophyly was also rejected at the 1% level by approximately unbiased and Shimodaira–Hasegawa tests where the “Hoplonymphidae” were constrained to be monophyletic and the tree re-optimized (see inset for this topology).

which this may occur. This is also supported by the fact that the glycocalyx in some protists is known to house receptor molecules that selectively accumulate specific metabolites from the surrounding medium (Hausmann, Hülsmann, and Radek 2003).

The linear pattern of bacteria on the surface indicates that most bacteria have actually grown there rather than having attached from the surrounding medium. The process of surface colonization following division or emergence from the resistant stage is therefore seeded by a small number of bacteria that grow to cover the surface. Presumably the underlying linear organization (rows of bacterial cells) that this should generate becomes somewhat obscured as the growing bacteria encounter one another, resulting in more random configurations (Fig. 1, 14). This may also depend in part on the relative speed of bacterial division related to protist cell expansion, and the degree to which attachment structures may allow for lateral displacement of surface bacteria on the protist cell surface. Bloodgood and Fitzharris (1976) did not observe bacterial surface symbionts in the process of division on trophozoites, and concluded they probably divide only when the protist host cell divides. However, we did observe signs of recent bacterial cell division on trophozoite surfaces—specifically bacterial cells that are apparently still conjoined, and are distinctly smaller (about half the length) of neighboring cells (Fig. 22, 25 ellipses). Hence, ongoing bacterial cell division seems to occur and obscures earlier linear organization.

Cytoplasmic protrusions from the protist cell surface may indicate a need—by at least one of the partners—for increased area for exchange of metabolites, but it may also be an indirect outcome of bacterial growth: if bacterial division outstrips any increase in size of the host, then growing chains of bacteria might push the surface up.

**Diversity and relationship of *Barbulanympha* and *Urinympha* according to SSU rRNA phylogeny.** If Hoplonymphidae were monophyletic, it would suggest that the formation of specialized cellular structures to house surface symbiotic bacteria might be a synapomorphy of this family. However, the basal position for *Hoplonympha* suggests that this feature might have arisen independently in *Hoplonympha* and the ancestor of *Barbulanympha* and *Urinympha*. Alternatively, it may be plesiomorphic in this group of Trichonymphida, retained by *Barbulanympha* and *Urinympha*, and lost in Spirotrichosomidae and Eucomonymphidae—in which bacterial surface symbionts are either lacking, or when present, differ from those on *Barbulanympha* and *Urinympha* in their morphology, much lower abundance and density, and arrangement (Carpenter et al. 2010; Carpenter and Keeling 2007; Noda et al. 2005).

#### ACKNOWLEDGMENTS

The authors thank Christine Nalepa for generously sharing collections of *C. punctulatus*, and Garnet Martens and the staff of the UBC Bioimaging Facility for technical assistance with electron microscopy. This work was supported by grants from the Natural Sciences and Engineering Research Council of Canada (227301) and AH was supported by a grant from the Tula Foundation to the Centre for Microbial Diversity and Evolution. P.J.K. is a Senior Scholar of the Michael Smith Foundation for Health Research and a Fellow of the Canadian Institute for Advanced Research. Work at Lawrence Livermore National Laboratory (writing portions of the manuscript by K.J.C.) was performed under the auspices of the U.S. Department of Energy under contract DE-AC52-07NA27344.

#### LITERATURE CITED

Bloodgood, R. A. & Fitzharris, T. P. 1976. Specific associations of prokaryotes with symbiotic flagellate protozoa from the hindgut of the

- termite *Reticulitermes* and the wood-eating roach *Cryptocercus*. *Cytobios*, **17**:103–122.
- Brugerolle, G. & Bordereau, C. 2004. The flagellates of the termite *Hodotermopsis sjoestedti* with special reference to *Hoplonympha*, *Holomastigotes* and *Trichomonoides trypanoides* n. comb. *Eur. J. Protistol.*, **40**:163–174.
- Brugerolle, G. & Lee, J. J. 2000. Phylum Parabasalia. In: Lee, J. J., Leedale, G. F. & Bradbury, P. (ed.), *An Illustrated Guide to the Protozoa*. 2nd ed. Allen Press Inc, Lawrence, KS. **2**:1196–1250.
- Carpenter, K. J. & Keeling, P. J. 2007. Morphology and phylogenetic position of *Eucomonympha inla* (Parabasalia: Hypermastigida). *J. Eukaryot. Microbiol.*, **54**:325–332.
- Carpenter, K. J., Chow, L. & Keeling, P. J. 2009. Morphology, phylogeny, and diversity of *Trichonympha* (Parabasalia: Hypermastigida) of the wood-feeding cockroach *Cryptocercus punctulatus*. *J. Eukaryot. Microbiol.*, **56**:305–313.
- Carpenter, K. J., Horak, A. & Keeling, P. J. 2010. Phylogenetic position and morphology of Spirotrichosomidae (Parabasalia): new evidence from *Leptospironympha* of *Cryptocercus punctulatus*. *Protist*, **161**:122–132.
- Carpenter, K. J., Waller, R. F. & Keeling, P. J. 2008. Surface morphology of *Saccinobaculus* (Oxymonadida): implications for character evolution and function in oxymonads. *Protist*, **159**:209–221.
- Cepicka, I., Hampl, V. & Kulda, J. 2010. Critical taxonomic revision of parabasalids with description of one new genus and three new species. *Protist*, **161**:400–433.
- Cleveland, L. R. 1951. Hormone-induced sexual cycles of flagellates. VII. One-division meiosis and autogamy without cell division in *Urinympha*. *J. Morph.*, **88**:385–439.
- Cleveland, L. R. & Grimstone, A. V. 1964. The fine structure of the flagellate *Mixotrichia paradoxa* and its associated microorganisms. *Proc. R. Soc.*, **159**:668–686.
- Cleveland, L. R., Hall, S. R., Sanders, E. P. & Collier, J. 1934. The wood-feeding roach *Cryptocercus*, its protozoa, and the symbiosis between protozoa and roach. *Mem. Am. Acad. Arts Sci.*, **17**:1–342.
- Everaerts, C., Maekawa, K., Farine, J. P., Shimada, K., Luyckx, P., Brossut, R. & Nalepa, C. A. 2008. The *Cryptocercus punctulatus* species complex (Dictyoptera: Cryptoceridae) in the eastern United States: comparison of cuticular hydrocarbons, chromosome number, and DNA sequences. *Mol. Phylogenet. Evol.*, **47**:950–959.
- Grassi, B. 1917. Flagellati viventi nei Termiti. *Mem. R. Accad. Lincei.*, **12**:331–394.
- Hausmann, K., Hülsmann, N. & Radek, R. 2003. Protistology. Schweizerbart'sche Verlagsbuchhandlung, Stuttgart, Germany.
- Hollande, A. & Carruette-Valentin, J. 1971. Les attractophores, l'induction du fuseau et la division cellulaire chez les Hypermastigines Étude infrastructurale et révision systématique des Trichonymphines et des Spirotrichonymphines. *Protistologica*, **7**:5–100.
- Hongoh, Y., Sharma, V. K., Prakash, T., Noda, S., Taylor, T. D., Kudo, T., Sakaki, Y., Toyoda, A., Hattori, M. & Ohkuma, M. 2008a. Complete genome of the uncultured termite group 1 bacteria in a single host protist cell. *Proc. Natl. Acad. Sci. USA*, **105**:5555–5560.
- Hongoh, Y., Sharma, V. K., Prakash, T., Noda, S., Toh, H., Taylor, T. D., Kudo, T., Sakaki, Y., Toyoda, A., Hattori, M. & Ohkuma, M. 2008b. Genome of an endosymbiont coupling N<sub>2</sub> fixation to cellulolysis within protist cells in termite gut. *Science*, **322**:1108–1109.
- Ikeda-Ohtsubo, W., Desai, M., Stingl, U. & Brune, A. 2007. Phylogenetic diversity of 'Endomicrobia' and their specific affiliation with termite gut flagellates. *Microbiology*, **153**:3458–3465.
- Keeling, P. J. 2002. Molecular phylogenetic position of *Trichomitopsis termopsidis* (Parabasalia) and evidence for the Trichomitopsiinae. *Eur. J. Protistol.*, **38**:279–286.
- Lartillot, N., Lepage, T. & Blanquart, S. 2009. PhyloBayes 3: a Bayesian software package for phylogenetic reconstruction and molecular dating. *Bioinformatics*, **25**:2286–2288.
- Leidy, J. 1877. On intestinal parasites of *Termes flavipes*. *Proc. Acad. Nat. Sci. Philadelphia*, **29**:146–149.
- Müller, M. 1993. The hydrogenosome. *J. Gen. Microbiol.*, **139**:2879–2889.
- Nakashima, K. I., Watanabe, H. & Azuma, J. I. 2002. Cellulase genes from the parabasalian symbiont *Pseudotrichonympha grassii* in the hindgut of the wood-feeding termite *Coptotermes formosanus*. *Cell. Mol. Life Sci.*, **59**:1554–1560.

- Nalepa, C. A., Luykx, P., Klass, K. D. & Deitz, L. L. 2002. Distribution of karyotypes of the *Cryptocercus punctulatus* species complex (Dictyoptera: Cryptocercidae) in the Southern Appalachians: relation to habitat and history. *Ann. Entomol. Soc. Am.*, **95**:276–287.
- Noda, S., Hongoh, Y., Sato, T. & Ohkuma, M. 2009. Complex coevolutionary history of symbiotic Bacteroidales bacteria of various protists in the gut of termites. *BMC Evol. Biol.*, **9**:158.
- Noda, S., Iida, T., Kitade, O., Nakajima, H., Kudo, T. & Ohkuma, M. 2005. Endosymbiotic Bacteroidales bacteria of the flagellated protist *Pseudotriconympha grassii* in the gut of the termite *Coptotermes formosanus*. *Appl. Environ. Microbiol.*, **71**:8811–8817.
- Noda, S., Inoue, T., Hongoh, Y., Kawai, M., Nalepa, C. A., Vongkaluang, C., Kudo, T. & Ohkuma, M. 2006. Identification and characterization of ectosymbionts of distinct lineages in Bacteroidales attached to flagellated protists in the gut of termites and a wood-feeding cockroach. *Environ. Microbiol.*, **8**:11–20.
- Noda, S., Kitade, O., Inoue, T., Kawai, M., Kanuka, M., Hiroshima, K., Hongoh, Y., Constantino, R., Uys, V., Zhong, J., Kudo, T. & Ohkuma, M. 2007. Cospeciation in the triplex symbiosis of termite gut protists (*Pseudotriconympha* spp.), their hosts, and their bacterial endosymbionts. *Mol. Ecol.*, **16**:1257–1266.
- Ohkuma, M. 2008. Symbioses of flagellates and prokaryotes in the gut of lower termites. *Trends Microbiol.*, **16**:345–352.
- Ohkuma, M. & Kudo, T. 1996. Phylogenetic diversity of the intestinal bacterial community in the termite *Reticulitermes speratus*. *Appl. Environ. Microbiol.*, **62**:461–468.
- Ohkuma, M., Noda, S., Hongoh, Y., Nalepa, C. A. & Inoue, T. 2009. Inheritance and diversification of symbiotic trichonymphid flagellates from a common ancestor of termites and the cockroach *Cryptocercus*. *Proc. Biol. Sci.*, **276**:239–245.
- Radek, R. & Tischendorf, G. 1999. Bacterial adhesion to different termite flagellates: ultrastructural and functional evidence for distinct molecular attachment modes. *Protoplasma*, **207**:43–53.
- Radek, R., Hausmann, K. & Breunig, A. 1992. Ectobiotic and endocytobiotic bacteria associated with the termite flagellate *Joenia-Annectens*. *Acta Protozoologica*, **31**:93–107.
- Ronquist, F. & Huelsenbeck, J. P. 2003. MrBayes 3: Bayesian phylogenetic inference under mixed models. *Bioinformatics*, **19**:1572–1574.
- Rother, A., Radek, R. & Hausmann, K. 1999. Characterization of surface structures covering termite flagellates of the family Oxymonadidae and ultrastructure of two oxymonad species, *Microrhopalodina multinucleata* and *Oxymonas* sp. *Eur. J. Protistol.*, **35**:1–16.
- Shimodaira, H. 2002. An approximately unbiased test of phylogenetic tree selection. *Syst. Biol.*, **51**:492–508.
- Shimodaira, H. & Hasegawa, M. 2001. CONSEL: for assessing the confidence of phylogenetic tree selection. *Bioinformatics*, **17**:1246–1247.
- Smith, H. E. & Armott, H. J. 1974. Epi- and endobiotic bacteria associated with *Pyrsonympha vertens*, a symbiotic protozoan of the termite *Reticulitermes flavipes*. *Trans. Am. Micros. Soc.*, **93**:180–194.
- Stamatakis, A. 2006. RAXML-VI-HPC: maximum likelihood-based phylogenetic analyses with thousands of taxa and mixed models. *Bioinformatics*, **22**:2688–2690.
- Stingl, U., Radek, R., Yang, H. & Brune, A. 2005. “Endomicrobia”: Cytoplasmic symbionts of termite gut protozoa form a separate phylum of prokaryotes. *Appl. Environ. Microbiol.*, **71**:1473–1479.
- Tamm, S. L. 1980. The ultrastructure of prokaryotic-eukaryotic cell junctions. *J. Cell. Sci.*, **44**:335–352.
- Todaka, N., Inoue, T., Saita, K., Ohkuma, M., Nalepa, C. A., Lenz, M., Kudo, T. & Moriya, S. 2010. Phylogenetic analysis of cellulolytic enzyme genes from representative lineages of termites and a related cockroach. *PLoS One*, **5**:e8636.
- Trager, W. 1934. The cultivation of a cellulose-digesting flagellate, *Trichomonas termopsidis*, and of certain other termite protozoa. *Biol. Bull.*, **66**:182–190.
- Yamin, M. A. 1979. Flagellates of the orders Trichomonadida Kirby, Oxymonadida Grasse, and Hypermastigida Grassi and Foa reported from lower termites (Isoptera Families Mastotermitidae, Kalotermitidae, Hodotermitidae, Termopsidae, Rhinotermitidae, and Serritermitidae) and from the wood-feeding roach *Cryptocercus* (Dictyoptera, Cryptocercidae). *Sociobiology*, **4**:3–119.
- Yamin, M. A. 1980. Cellulose metabolism by the termite flagellate *Trichomitopsis termopsidis*. *Appl. Environ. Microbiol.*, **39**:859–863.

Received: 02/17/11, 04/25/11; accepted: 04/27/11